ELECTRONIC RESEARCH ARCHIVE
Volume **29**, Number **5**, November **2021**

doi:10.3934/era.2021035
pp. **3227–3241**

ENHANCEMENT OF GAMMA OSCILLATIONS IN E/I NEURAL NETWORKS BY INCREASE OF DIFFERENCE BETWEEN EXTERNAL INPUTS

Xiaochun Gu, Fang Han*, Zhijie Wang* and Kaleem Kashif

College of Information Science and Technology
Donghua University
Shanghai 201620, China

Wenlian Lu

Key Laboratory of Computational Neuroscience and Brain-Inspired Intelligence
Ministry of Education, Fudan University
Shanghai 200433, China

Abstract. Experimental observations suggest that gamma oscillations are enhanced by the increase of the difference between the components of external stimuli. To explain these experimental observations, we firstly construct a small excitatory/inhibitory (E/I) neural network of IAF neurons with external current input to E-neuron population differing from that to I-neuron population. Simulation results show that the greater the difference between the external inputs to excitatory and inhibitory neurons, the stronger gamma oscillations in the small E/I neural network. Furthermore, we construct a large-scale complicated neural network with multi-layer columns to explore gamma oscillations regulated by external stimuli which are simulated by using a novel CUDA-based algorithm. It is further found that gamma oscillations can be caused and enhanced by the difference between the external inputs in a large-scale neural network with a complicated structure. These results are consistent with the existing experimental findings well.

1. **Introduction.** Neuronal oscillations in the gamma range (30-90Hz) appearing in different areas of the brain are thought to carry important information for cognitive and perception functions [7, 3]. Experimental observations have suggested that gamma oscillations can be enhanced by the increase of the difference between the components of an external stimulus (for example, the increase of illumination contrast of a grating stimulus) in the visual cortex. Adjamian et al. [1] showed that gamma activity was stronger in response to a higher difference in luminance of gratings. Henrie et al. [6] found that the gamma-band power in the V1 zone was strengthened with the increase of the difference between light and dark areas of the stimulus. Saleem et al. [15] suggested that the narrowband gamma oscillation was enhanced with the difference in light intensity in the mouse visual cortex.

The above experimental researches can be summarized that gamma oscillations are strengthened by the increase of the difference between external inputs to neurons, i.e. if there are two types of external inputs to a neural system, the greater

2020 *Mathematics Subject Classification.* Primary: 92B20, 92C20; Secondary: 92-10.
Key words and phrases. Gamma oscillations, E/I neural network, large-scale, stimulus.
* Corresponding author: Fang Han and Zhijie Wang.

the difference between the two inputs is, the stronger the gamma oscillation of the system is. However, this is counterintuitive and different from the conventional understanding: the neural network is prone to synchronize [19, 5, 20] and generate gamma oscillations if neurons are uniform and the external inputs to them are equal. Therefore, it is necessary to establish relevant models of a biological neural network to reproduce the experimental observations and investigate how gamma oscillations change with the variation of external inputs.

In this paper, we firstly establish a small excitatory/inhibitory (E/I) neuronal network [11, 16] composing of Integrate-and-Fire (IAF) neurons with external current inputs to E-neurons differing from that to I-neurons. The simulation results of the small E/I network show that gamma oscillations are enhanced with the increase of the difference between the external inputs to E- and I- neurons, which are consistent with the biological experimental results well. Then we further study gamma oscillations in a large-scale neural network with complicated structure by using a novel CUDA-based algorithm for its simulation. It is further found that gamma oscillations can be caused and enhanced by the difference between the external inputs in large-scale neural networks with complicated structures.

2. **Enhancement of Gamma oscillations in small E/I neural network.**

2.1. **Small E/I neural network model.**

In this section, we will study gamma oscillations regulated by external inputs in a small E/I neural network. Both the excitatory neurons (E-neurons) and inhibitory neurons (I-neurons) in this small network are described by Integrate-and-Fire (IAF) model neurons [14] and conductance-based synapse model [4]. IAF model neurons can be described by Eq. 1:

$$\tau \frac{\mathrm{d}V_i}{\mathrm{d}t} = -(V_i - \mathrm{V_L}) + R(\sum_{j=1, j\neq i}^{N} I_{ij}^{\mathrm{syn}} + I^{\mathrm{ext}}) \tag{1}$$

where V_i represents the membrane potential of neuron i, τ is the membrane time constant, V_{L} is the equilibrium potential of leakage ions, R is the membrane resistance, I_{ij}^{syn} is the synaptic current transmitted from neuron j to neuron i, N denotes the number of the neurons in the network, and I^{ext} is the external stimuli of neuron i.

The conductance-based synapse model is described as follows:

$$\begin{cases} I_{ij}^{\mathrm{syn}} = g_{\max} s_{ij}(V_i - E_{\mathrm{syn}}), \\ \frac{\mathrm{d}s_{ij}}{\mathrm{d}t} = \alpha F(V_j)(1 - s_{ij}) - \beta s_{ij} \end{cases} \tag{2}$$

where $g_{\max}$ is the maximum conductance of the synapse (the synaptic weight), E_{syn} denotes the reverse potential of the synapse, s_{ij} denotes the opening level of the synaptic ion channel gate of neuron j connecting to neuron i, α is the gate enhancement factor and β is the gate decay factor, V_j is the membrane potential of presynaptic neuron j. After presynaptic neuron j is discharged, the resulting action potential reaches the synapse after a certain time (synaptic delay) [21] and $F(V_j) = 1$, or else $F(V_j) = 0$.

Assume that the step length is Δt, the model network can be described by the following discrete equations for each time step $t_1 \to t_2 (t_2 = t_1 + \Delta t)$ [13]:

$$\begin{cases} V_i(t_2) = V_i(t_1) + \dfrac{\Delta t}{\tau}(-V_i(t_1) + V_{\mathrm{L}} + R(\sum_{j=1}^{N} I_{ij}^{\mathrm{syn}}(t_1) + I^{\mathrm{ext}}) \\ I_{ij}^{\mathrm{syn}}(t_1) = g_{\max} s_{ij}(t_1)(V_i(t_1) - E_{\mathrm{syn}}) \qquad (j \neq i) \\ s_{ij}(t_2) = s_{ij}(t_1) + (\alpha \cdot F(V_j) \cdot (1 - s_{ij}(t_1)) - \beta \cdot s_{ij}(t_1))\Delta t \end{cases} \tag{3}$$

The small E/I network consists of 400 excitatory neurons and 100 inhibitory neurons with all-to-all connections (see Fig. 1). The parameters $g_{\max}$, E_{syn}, τ for E neurons are set as 0.00048, $0mV$, $5ms$, and those for I neurons are set as 0.012, $-75mV$, $1ms$, respectively [11, 4]. The parameters V_{L}, R, α, β are set as $V_{\mathrm{L}} = -65mV$, $R = 10k\Omega$, $\alpha = 0.9$, $\beta = 0.003$ for both E- and I- neurons. The spiking threshold potentials V_{th} for E- and I- neurons are both set as $-45mV$. When the membrane potential V_i reaches the threshold potential, neuron i emits a pulse (action potential) and then V_i resets to the resting membrane potential V_{reset}($V_{\mathrm{reset}} = -65mV$ for both E- and I- neurons). The synaptic delay is set as $3ms$.

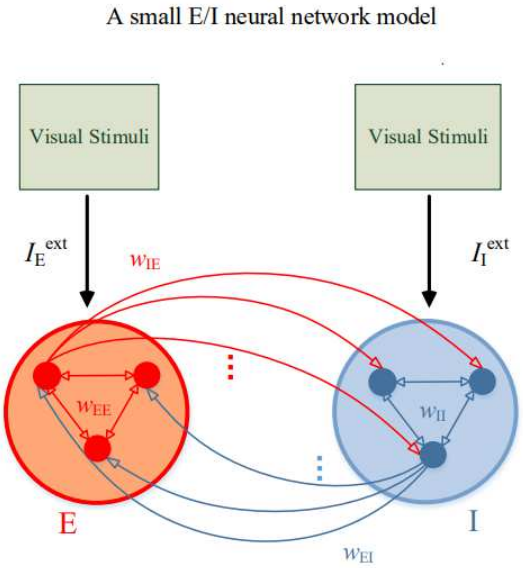

FIGURE 1. The structure of the small E/I network with external stimuli. Wiring among E- and I- neurons are all-to-all and only three cells of the E-neuron population (red dots) and I-neuron population (blue dots) are depicted here. Directed wiring is red for excitatory and blue for inhibitory connections. w_{EE}, w_{II}, w_{EI} and w_{IE} are the synaptic weights ($g_{\max}$) of E to E, I to I, I to E, and E to I connections, respectively.

2.2. **Simulation methods and results.** Excitatory neuron population and inhibitory neuron population are assumed to receive different inputs mapped from the external stimulus, due to the different receptive fields of them and the non-uniform spatial distribution of the stimulus (for example, the different distributions

of the gray values of pixels in a visual stimulus) [8]. Different values, $S1$ and $S2$, are thereby assumed to be the external current inputs to E- and I- neuron populations, respectively [8] (i.e. $I_{\mathrm{E}}^{\mathrm{ext}} = S1$ for excitatory neuron population and $I_{\mathrm{I}}^{\mathrm{ext}} = S2$ for inhibitory neuron population). Firstly, we simulated the network with the typical inputs of $S1$ and $S2$ to observe in which conditions the small network can generate gamma oscillations. Then we regulate the gamma oscillations by increasing the difference between $S1$ and $S2$ with the following two cases: (i) increase parameter $S1$ gradually from 0 to 1.0 but keeping parameter $S2$ unchanged; (ii) increase parameter $S2$ gradually from 0 to 1.0 but keeping parameter $S1$ unchanged.

The network simulation and data analysis are done with MATLAB 2012a. The biological time of this small E/I network is set as 1s and the time step is 0.01ms. Before our simulations, we have made the excitatory synaptic currents for each neuron equal to its inhibitory synaptic currents by adjusting the parameters of the network. Thereby, there is no net synaptic currents to the neurons in the network under the initial conditions of the simulations. Firstly, we simulated the small network under two typical inputs ($S1 = 0.6, S2 = 0$ and $S2 = 0.2, S1 = 0$), then plotted separately the spiking times of neurons, the population spiking activities, and the power spectrums as shown in Fig. 2 and Fig. 3. Fig. 2(b) and Fig. 3(b) are the average population activities which are calculated from Fig. 2(a) and Fig. 3(a) respectively by counting spikes in time bins of width 1ms and convolving with a Gaussian of width $100ms$. The power spectrums of the average population activities in Fig. 2(c) and Fig. 3(c) are calculated using the method of FFT transform [2]. Oscillation frequency is defined as the frequency component whose amplitude is largest among all frequency components of the average population activities. The oscillation power is defined as the power of the oscillation frequency. Thereby,the peak of a distinct bump in the power spectrum is the oscillation power and the frequency at this peak is the oscillation frequency. The peak frequency at the peak power in Fig. 2(c) is near 48Hz and the peak frequency in Fig. 3(c) is near 47Hz which are both within the gamma frequency band. The high peaks of distinct bumps both in Fig. 2(c) and Fig. 3(c) imply that the strong gamma oscillations can be caused when E- and I- neurons receive different external inputs.

It is worthy of noting that we use the relative value of the power (called ***Relative Power*** here), which is defined by ***Relative Power=Power/PowerSUM*** (***Power*** stands for the power of each frequency component and ***PowerSUM*** is the sum of the power of all frequencies in the power spectrum), to represent the magnitude of power in the power spectrum. ***Relative Power*** is more reasonable than the absolute value of the power of a frequency component since the absolute value of the power depends not only on the strength of the oscillation of the corresponding frequency component but also on the firing rate of neurons in a neuronal network.

How the gamma oscillations generated in the small E/I network are regulated by the difference between $S1$ and $S2$ in the two regulation cases is summarized in Fig. 4. In the first case, when $S1$ (the external inputs to E neurons) is increased from 0 to 1.0, i.e. the difference between the inputs to E- and I- neurons is increased from 0 to 1.0, the peak power of the gamma oscillations increases gradually (the green curve). In the second case, the power becomes stronger and stronger (the blue curve) as $S2$ (the external inputs to I neurons) is increased from 0 to 1.0, i.e. the difference between the inputs to E- and I- neurons is also increased from 0 to 1.0. The more upward trend for the case of the increase of $S2$ (the blue curve) indicates

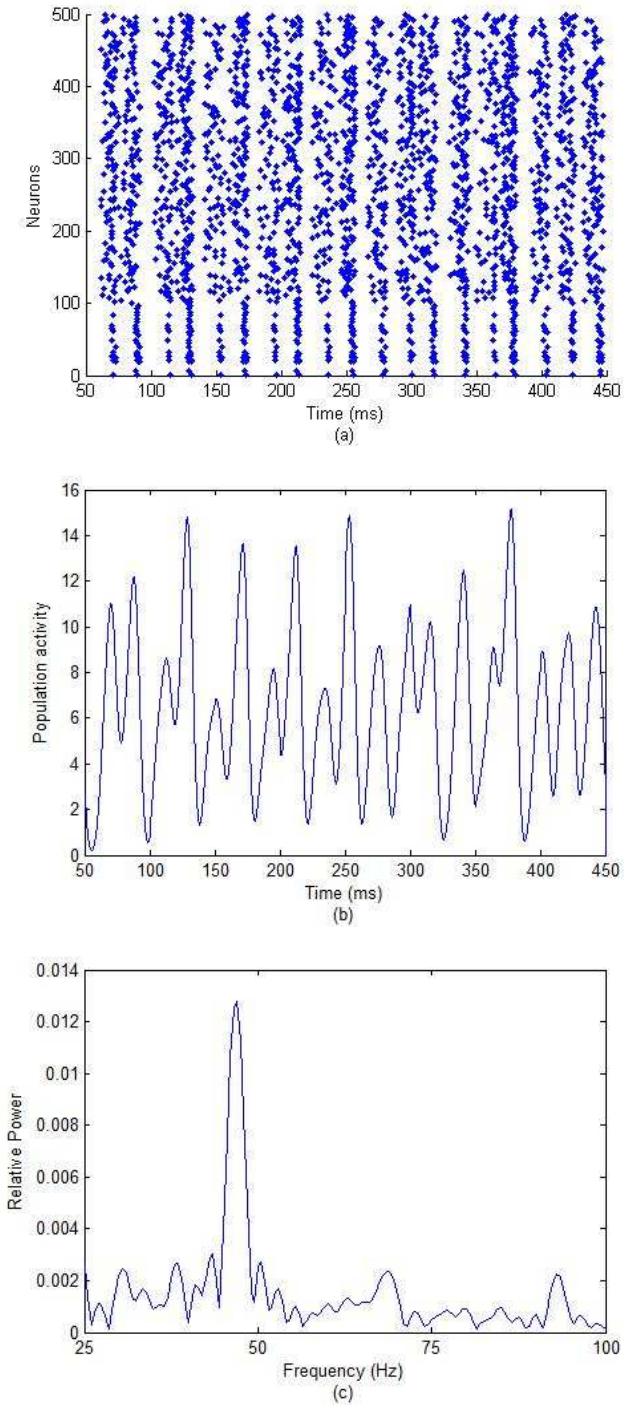

FIGURE 2. Gamma oscillations are caused by the typical input that $S1$ is 0.6 and $S2$ is zero (50ms-450ms in a 1s simulation). (a) Raster plots of the spiking times of neurons. (b) Average population activity. (c) The power spectrum of the population activity.

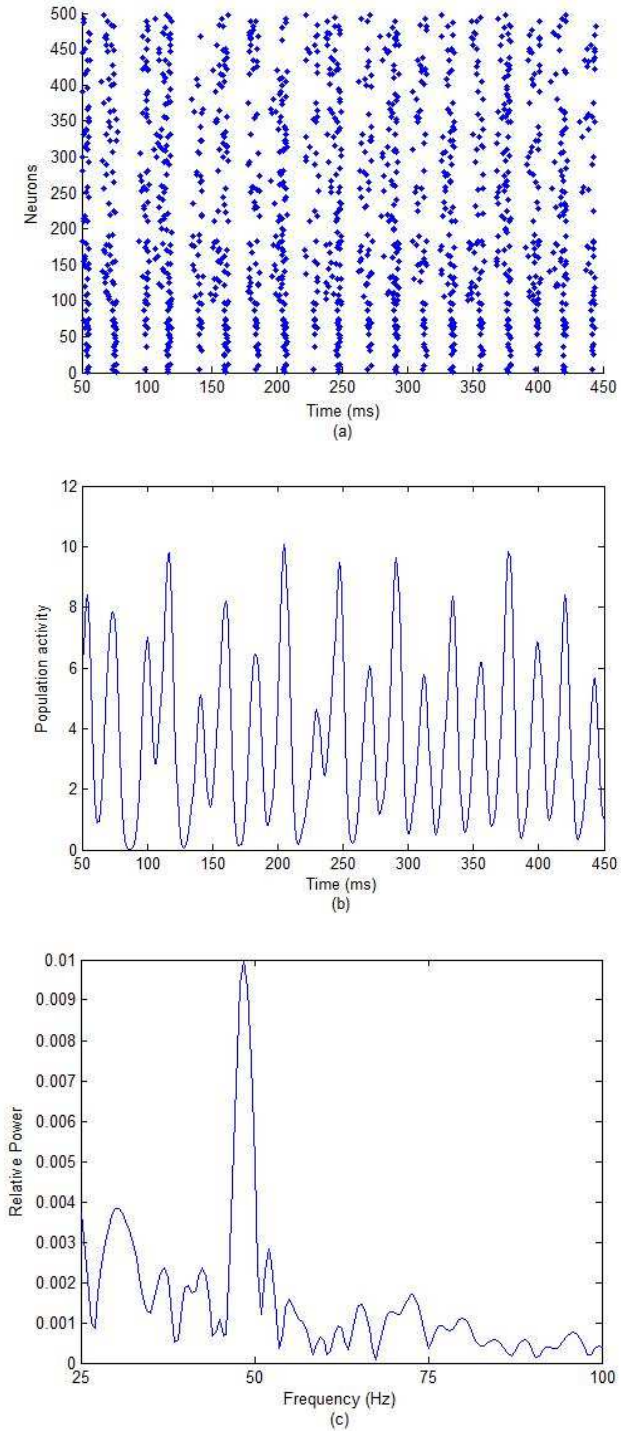

FIGURE 3. Gamma oscillations are caused by the typical input that $S2$ is 0.2 and $S1$ is zero (50ms-450ms in a 1s simulation). (a) Raster plots of the spiking times of neurons. (b) Average population activity. (c) The power spectrum of the population activity.

that the gamma oscillations of the network are more sensitive to the changes of the inputs to I neurons.

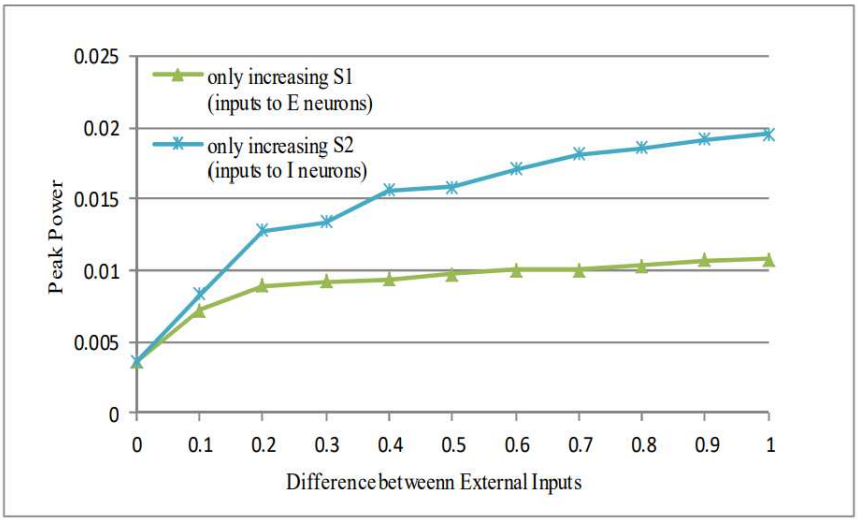

FIGURE 4. Increase of the peak power of gamma oscillations in the small E/I neural network with the increasing of the difference between $S1$ and $S2$. The increase of the peak power in the second case (blue curve) is more evident than that in the first case (green curve).

In short, the simulation results of the small E/I network show that gamma oscillations can be caused by the difference between the external inputs to excitatory and inhibitory neurons and get stronger with the increasing of the input difference, which is consistent well with what observed in existing biological experimental findings. However, a small neural network model cannot fully describe the actual biological nervous system that contains a large number of neurons and has a complex network structure. Therefore, we will next construct a large-scale neural network model with a complicated structure to further explore how the intensity of gamma oscillations change with external stimuli.

3. **Enhancement of gamma oscillations in large-scale neural network with complicated structure.**

3.1. **Large-scale neural network with complicated structure.**

According to the network structure's complexity of the real biological neural systems in the brain, we first construct a column composed of multiple layers and then use 10 multi-layer columns to set up a large-scale neural network model [9, 12]. Each column is composed of four network layers, which are layer 2/3, layer 4, layer 5, and layer 6, respectively, as shown in Fig. 5. There are 8 different types of neurons in a single column including E23, I23, E4, I4, E5, I5, E6, and I6, where "E" and "I" represent excitatory neurons and inhibitory neurons respectively and the number following them represents the layer. Figure 5 shows intra-layer and inter-layer neuron connections within a single column according to Table 2 [11], wherein red circles indicate

excitatory neuron populations and excitatory connections are depicted by red directed wiring, blue circles indicate inhibitory neuron populations, and inhibitory connections are depicted by blue directed wiring. $I_{\mathrm{E}}^{\mathrm{ext}}$ and $I_{\mathrm{I}}^{\mathrm{ext}}$ (black wiring in Fig. 5) are external inputs to E and to I neurons respectively in each column.

The excitatory and inhibitory neurons in this large-scale complicated network are both described by Integrate-and-Fire (IAF) neurons (see Eq. 1) and their synapses are also described by the conductance-based synapse model (see Eq. 2). In the following simulations, the neuron parameters within columns are listed in Table 1 [4] and a single column contains $1,000$ neurons including 800 excitatory neurons and 200 inhibitory neurons. In a column, the connection probability between neurons is 50% and the connection types and parameters of neurons are listed in Table 2. The connection probability of neurons connected between columns is 7% and the connection types and parameters are listed in Table 3 [11].

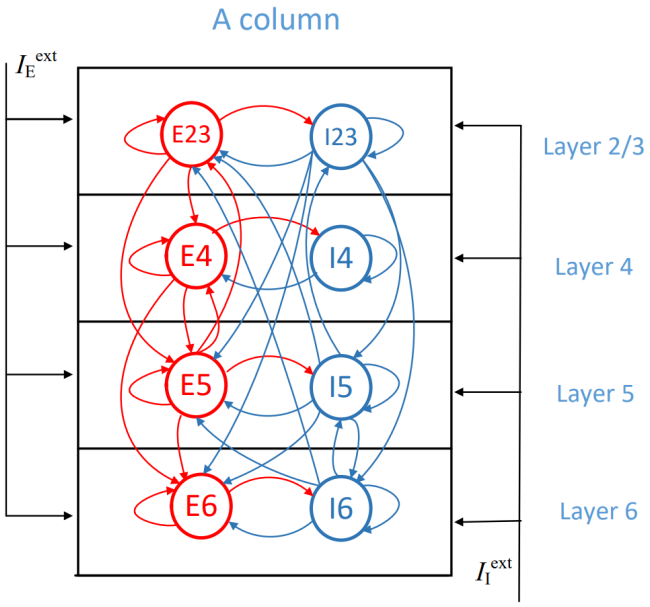

FIGURE 5. Intra-layer and inter-layer connections in a single column.

3.2. **Parallel simulations and results.** Based on the existing CUDA parallel algorithm [17] combined with a synapse optimization algorithm [18] which were proposed to implement the simulation for a large-scale neural network with simple structure, we design a novel CUDA-based algorithm to simulate the large-scale complicated neural network with multi-layer columns and the simulation framework is shown in Fig. 6. The red dashed box on the left of Fig. 6 shows the establishment of the complicated column structure of the large-scale network, including the initialization of connection probability between neurons, the initialization of parameters for each type of neurons according to Table 1 , the establishment of neuron connections within columns and between columns and parameter settings of $g_{\max}$ and d according to Table 2 and Table 3. The pseudo-code

TABLE 1. Parameters and counts of different types of neurons within a column

Type	N	$V_{\text{th}}(mV)$	$V_{\text{reset}}(mV)$	$E_{\text{syn}}(mV)$	$\tau(ms)$	$R(k\Omega)$	$V_{\text{L}}(mV)$
E23	200	-47	-65	0	5	10	-65
I23	50	-45	-65	-75	1	10	-65
E4	200	-47	-65	0	5	10	-65
I4	50	-45	-65	-75	1	10	-65
E5	200	-47	-65	0	5	10	-65
I5	50	-45	-65	-75	1	10	-65
E6	200	-47	-65	0	5	10	-65
I6	50	-45	-65	-75	1	10	-65

TABLE 2. Connection Types and parameters of neurons within a column

presynaptic neuron	postsynaptic neuron	α	β	$g_{\max}$	$d(ms)$
E23	E23,E4,E5,I23	0.9	0.003	0.004	2
I23	E23,E5,E6,I23, I5,I6	0.9	0.003	0.05	1
E4	E4,E5,E6,I4	0.9	0.003	0.004	2
I4	E4,I4	0.9	0.003	0.05	1
E5	E23,E4,E5, E6,I5	0.9	0.003	0.004	2
I5	E23,E5,E6,I23, I5,I6	0.9	0.003	0.05	1
E6	E6,I6	0.9	0.003	0.004	2
I6	E23,E5,E6,I5,I6	0.9	0.003	0.05	1

TABLE 3. Connection types and parameters of neurons between columns

presynaptic neuron	postsynaptic neuron	α	β	$g_{\max}$	$d(ms)$
E23	I23	0.8	0.001	0.98	1
E4	I4	0.8	0.001	0.98	1
E5	E5	0.8	0.001	0.16	1
E5	I5	0.8	0.001	0.98	1
E5	E23	0.8	0.001	0.16	1
E5	I23	0.8	0.001	0.98	1
E6	I6	0.8	0.001	0.98	1

of constructing the complicated network structure is shown in Algorithm 1 (see Fig. 7). The flow chart under the red dashed box in Fig. 6 illustrates the computations of neuron states (the synaptic current I_{ij}^{syn} and the membrane potential V_i), of which the algorithm is similar to that proposed in [17]. For the novel CUDA-based algorithm to simulate a large-scale network with N neurons, we can use a one-dimensional grid (kernel) consisting of $N/blockDim$ (number of neurons/block size) one-dimensional blocks and 1024 one-dimensional threads in each block (i.e., the block size is 1024) on GPU [10]. The index number of each block is $blockIdx.x = 0, 1, ..., m, ..., (N/1024 - 1)$ and the index number of each thread in each block is $threadIdx.x = 0, 1, ..., m, ..., 1023$. So the index number of each

neuron mapped to a single thread is $blockIdx.x * 1024 + threadIdx.x$,e.g., the state $0, 1$ calculations of the $(m * 1024 + n)$th neuron at all time steps will be executed in the nth thread of the mth block. The CUDA-based parallel architecture for implementing the state calculations of all neurons in the simulations of the large-scale complicated network with N neurons is shown on the right of Fig. 6.

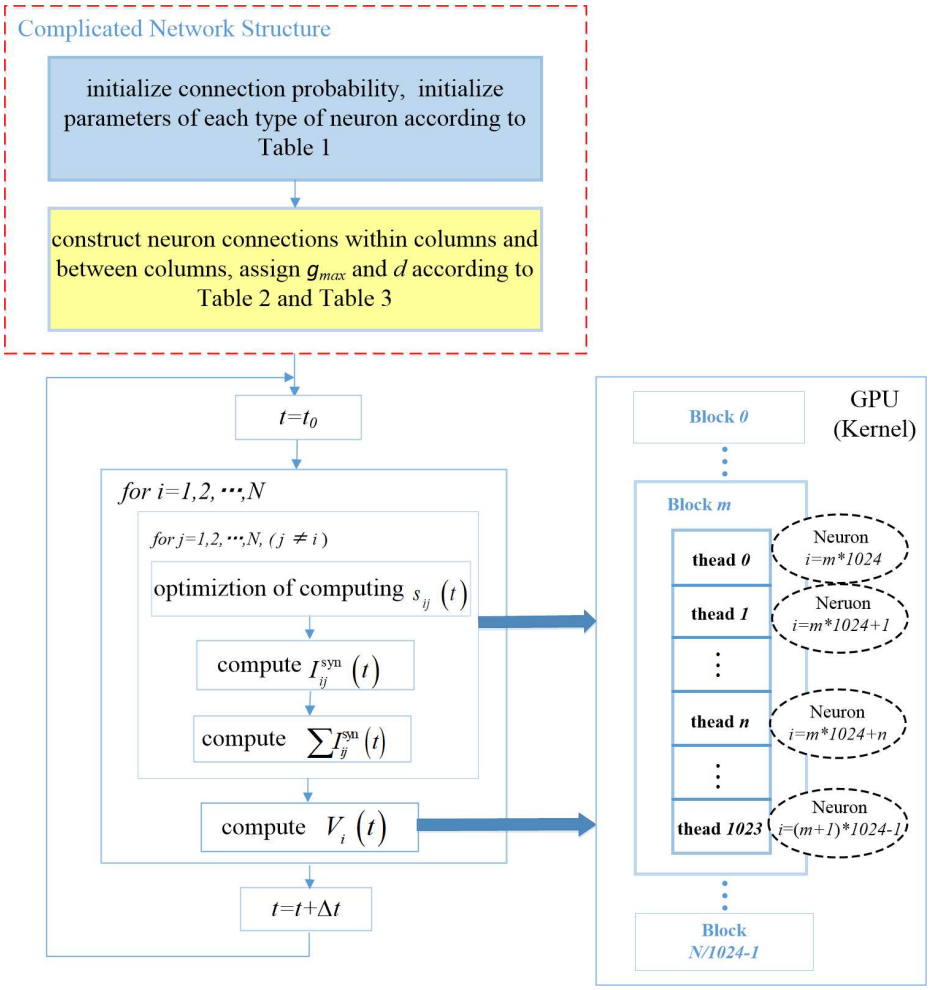

FIGURE 6. The framework of simulation for the large-scale complicated network with multi-layer columns. t_0 is the initial time. Δt is the time step.

Therefore, we used a one-dimensional grid (kernel) consisting of 10 one-dimensional blocks and 1024 one-dimensional threads in each block on GPU to simulate our large-scale complicated neural network with 10 columns. The biological time of the network is set as $0.5s$ and the simulation time step is set as $0.01ms$. The software environment is 64-bit Windows 10, VS2015 programming environment, C++ programming language, and CUDA-based parallel computing platform. The hardware environment is INTEL i7-7700HQ (dual-core), NVIDIA GeForce GTX

Algorithm 1 The program of constructing complicated network wtih multi-layer column structure

// initialize connection probability between neurons
unsigned int $m\_uiNumCell\_per\_column$
unsigned int idx_column, jdx_column
unsigned int $ii\_idx\_column = idx\_column * m\_uiNumCell\_per\_column$
unsigned int $jj\_jdx\_column = jdx\_column * m\_uiNumCell\_per\_column$
for each pair of neuron (i, j), **do**
  define the global id:*_LocIJ(ii_idx_column + i, jj_jdx_column + j)*
  if $idx\_column = jdx\_column$, **then**
    if $i \neq j$, **then**
    set the connection probability, $m\_pfwire[\_LocIJ(ii\_idx\_column + i, jj\_jdx\_column + j)] = 50\%$
    end if
  else
    set the connection probability, $m\_pfwire[\_LocIJ(ii\_idx\_column + i, jj\_jdx\_column + j)] = 7\%$
  end if
end for
// assign parameters to each type of neuron
load parameters from Table 1
for the ith neuron in the jth column , **do**
  define the layer labels corresponding to each type of neuron: $m\_pLayerForCell[i * m\_uiNumCell\_per\_column + j]$
  assign V_{reset}, V_{th}, τ, E_{syn}, R according to Table 1
  initialize s_0, V_0
end for
// set g_{max} and d between interconnected neurons
for each pair of neuron (i, j), **do**
  if $idx\_column = jdx\_column$, **then**
  find out the interconnected (i, j), define the global id:*_LocIJ(ii_idxcolum + i, jj_jdx_column + j)*
  assign g_{max} and d according to Table 2
  else
  find out the interconnected (i, j), define the global id:*_LocIJ(ii_idxcolum + i, jj_jdx_column + j)*
  assign g_{max} and d according to Table 3
  end if
end for

FIGURE 7. The pseudo-code of constructing the multi-layer column structure of the large-scale complicated network. The variable $m\_uiNumCell\_per\_column$ denotes the number of neurons in each column, the variables idx_column, and jdx_column denote the IDs of columns and the variables ii_idx_column and jj_jdx_column denote the IDs of neurons.

1060 (6GB). Similar to the simulation methods of the small network in Section 2.2, we first simulate the large-scale network with the typical inputs of $S1$ and $S2$ ($I_{\mathrm{E}}^{\mathrm{ext}} = S1$, $I_{\mathrm{I}}^{\mathrm{ext}} = S2$) to observe whether gamma oscillations can be generated

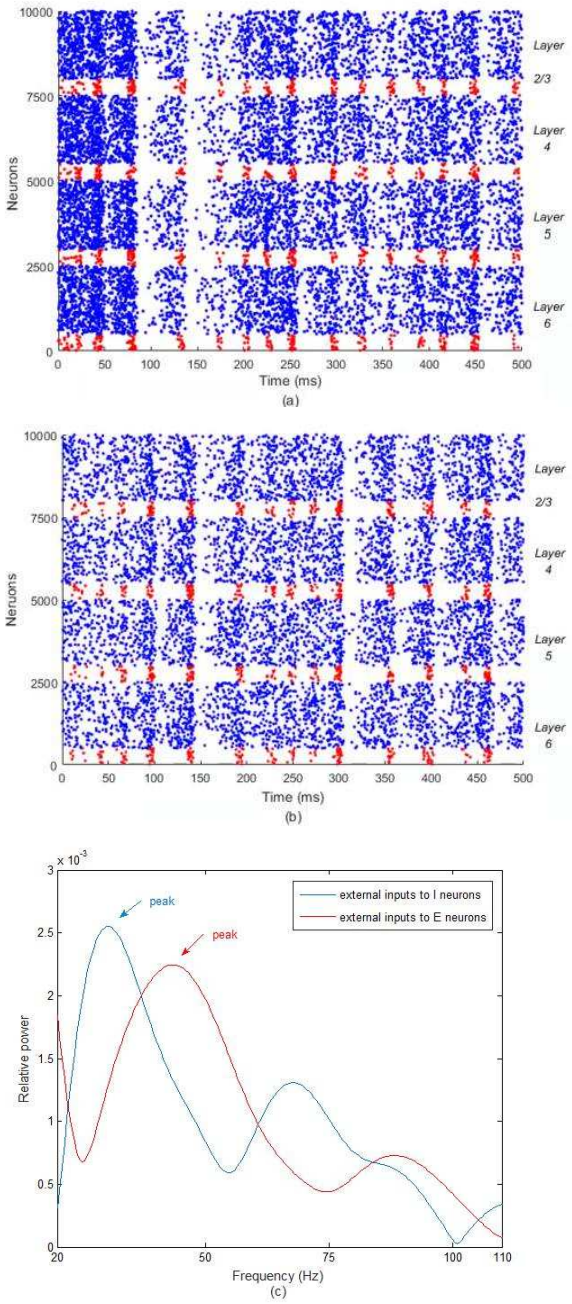

FIGURE 8. Gamma oscillations are generated in the large-scale complicated neural network. (a) Raster plots of the spiking times of neurons in each layer of columns when $S1 = 0.3, S2 = 0$. (b) Raster plots of the spiking times of neurons in each layer of columns when $S1 = 0, S2 = 0.3$. (c) Power spectrums of average population activities with the two input cases.

in the large-scale complicated neural network. The method of data analysis is similar to that of the small network and the simulation results are shown in Fig. 8 which are plotted in MATLAB 2010a. Figure 8(a) and Figure 8(b) show separately the raster plots of the spiking times of neurons in each layer of columns when $S1 = 0.3, S2 = 0$ and when $S1 = 0, S2 = 0.3$ (red dots represent the discharges of inhibitory neurons and blue dots represent the discharges of excitatory neurons). It is found that the periodic discharges of neurons are both generated in the large-scale complicated network. Figure 8(c) shows the power spectrums corresponding to Fig. 8(a) (red curve) and Fig. 8(b) (blue curve), respectively. We can find from Fig. 8(c) that there are both distinct peaks implying that the large-scale network generates obvious oscillations when E- and I- neurons receive different external inputs, and their dominant frequencies at the peaks belong to the gamma frequency band (30Hz-90Hz).

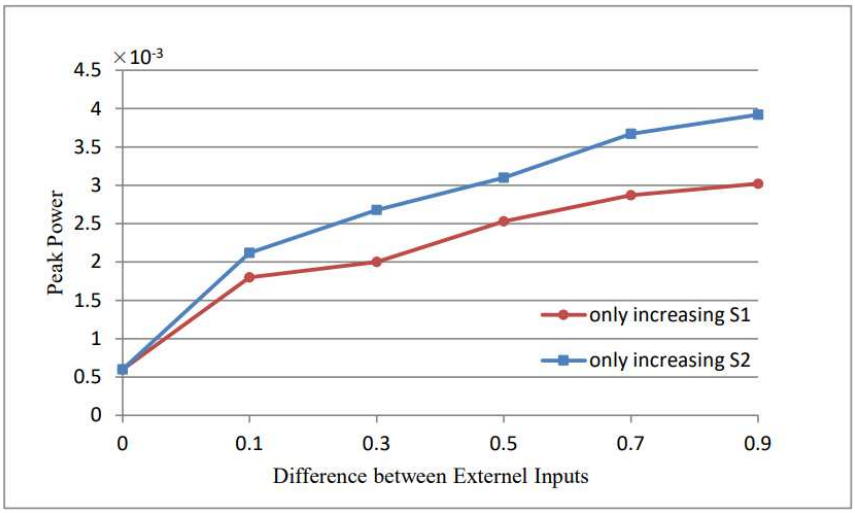

FIGURE 9. Increase of the peak power of gamma oscillations in the large-scale complicated network with the increasing of the difference between $S1$ and $S2$.

Next, we regulate the large-scale complicated network to observe how the peak power of the gamma oscillations change by increasing the input difference between $S1$ and $S2$ with the two regulation cases similar to the regulation method proposed in Section 2.2. In the first case, the peak power of the gamma oscillation increases gradually as $S1$ is increased from 0 to 1.0 (i.e., the input difference is increased from 0 to 1.0). In the second case, the peak power also gets strong gradually as $S2$ is increased from 0 to 1.0 (i.e., the input difference is increased from 0 to 1.0). Therefore,we can summarize that the peak power of gamma oscillations increases when the difference between the inputs to E- and I- neurons gradually increases from 0.1 to 1.0 according to a large amount of data obtained through many simulations, the results of which are shown in Fig. 9.

In short, the simulation results show that gamma oscillations can also be caused by the difference between the external inputs to excitatory and inhibitory neurons and get stronger with the increasing of the input difference in the large-scale neural

network with complicated structure, which are consistent with the existing biological experimental findings.

4. **Conclusion.** To explain the biological experimental observations that gamma oscillations are enhanced by the increase of the difference between the components of external stimuli (e.g., the increase of illumination contrast of a grating stimulus), we firstly construct a small excitatory/inhibitory (E/I) neural network consisting of IAF neurons with different external inputs to E- and I- neuron populations (E- and I- neurons have different receptive fields, thereby have different external inputs if there is difference between the external stimuli). We study the small E/I network with two different regulation cases and the simulation results show that the greater the difference between the inputs to E- and I- neuron populations is, the stronger the gamma oscillation is. Furthermore, a large-scale complicated neural network with multi-layer columns is constructed to explore gamma oscillations by using a novel CUDA-based algorithm for simulation. We further find that gamma oscillations can be caused and enhanced by the difference between the external inputs in a large-scale neural network with a complicated structure. The results of this paper are consistent well with the biological experimental observations, which is helpful for understanding the mechanism of enhancement of gamma oscillations by external stimuli. In the future,we will add the number of columns,the type and number of neurons to further expand the complicated network scale to study gamma oscillations.Moreover,we will further explore the cognitive funcitons of gamma oscillations with our models.

Acknowledgment. This work was supported by the National Natural Science Foundation of China (Grants Nos. 11972115, 11572084), Shanghai Municipal Science and Technology Major Project (No.2018SHZDZX01), Key Laboratory of Computational Neuroscience and Brain-Inspired Intelligence (LCNBI), and ZJLab.

REFERENCES

[1] P. Adjamian, A. Hadjipapas, G. R. Barnes, A. Hillebrand and I. E. Holliday, Induced gamma activity in primary visual cortex is related to luminance and not color contrast: An MEG study, *Journal of Vision*, **8** (2008), 1–7.

[2] A. M. Bastos, F. Briggs, H. J. Alitto, G. R. Mangun and W. M. Usrey, Simultaneous recordings from the primary visual cortex and lateral geniculate nucleus reveal rhythmic interactions and a cortical source for gamma-band oscillations, *Journal of Neuroscience*, **34** (2014), 7639–7644.

[3] G. Buzsáki and X.-J. Wang, Mechanisms of gamma oscillations, *Annu. Rev. Neurosci*, **35** (2012), 203–225.

[4] P. Dayan and L. F. Abbott, Theoretical Neuroscience: Computational and Mathematical Modeling of Neural Systems, Cambridge: MIT Press, 2001.

[5] P. Guiraud and E. Tanre, Stability of synchronization under stochastic perturbations in leaky integrate and fire neural networks of finite size, *Discrete Contin. Dyn. Syst. Ser. B*, **24** (2019), 5183–5201.

[6] J. A. Henrie and R. Shapley, LFP power spectra in V1 cortex: The graded effect of stimulus contrast, *Journal of Neurophysiology*, **94** (2005), 479–490.

[7] J. F. Hipp, A. K. Engel and M. Siegel, Oscillatory synchronization in large-scale cortical networks predicts perception, *Neuron*, **69** (2011), 387–396.

[8] M. P. Jadi and T. J. Sejnowski, Cortical oscillations arise from contextual interactions that regulate sparse coding, *Proc. Nat. Acad. Sci. USA*, **111** (2014), 6780–6785.

[9] V. B. Mountcastle, The columnar organization of the neocortex, *Brain*, **120** (1997), 701–722.

[10] J. M. Nageswaran, N. Dutt, J. L. Krichmar et al., A configurable simulation environment for the efficient simulation of large-scale spiking neural networks on graphics processors, *Neural Networks*, **22** (2009), 791–800.

[11] S. A. Neymotin, H. Lee, E. Park, A. A. Fenton and W. W. Lytton, Emergence of physiological oscillation frequencies in a computer model of neocortex, *Front. Comput. Neurosci.*, **5** (2011), 19.
[12] C. C. H. Petersen and B. Sakmann, Functionally independent columns of rat somatosensory barrel cortex revealed with voltage-sensitive dye imaging, *Journal of Neuroscience*, **21** (2001), 8435–8446.
[13] W. H. Press, S. A. Teukolsky and W. T. Vetterling, Numerical recipes in C: The art of scientific computing, *IEEE Concurrency*, **6** (1992), 79.
[14] L. Sacerdote and M. T. Giraudo, Stochastic Integrate and Fire Models: A review on mathematical methods and their applications, *Stochastic biomathematical models*, Lecture Notes in Math., Math. Biosci. Subser., Springer, Heidelberg, **2058** (2013), 99–148.
[15] A. B. Saleem, A. D. Lien, M. Krumin, B. Haider, M. R. Rosón, A. Ayaz, K. Reinhold, L. Busses, M. Carandini and K. D. Harris, Subcortical source and modulation of the narrowband gamma oscillation in mouse visual cortex, *Neuron*, **93** (2017), 315–322.
[16] E. Wallace, M. Benayoun, W. van Drongelen and J. D. Cowan, Emergent oscillations in networks of stochastic Spiking Neurons, *PLOS ONE*, **6** (2011).
[17] Z. J. Wang, X. Peng and F. Han, A novel parallel clock-driven algorithm for simulation of neuronal networks based on virtual synapse, *Simulation*, **94** (2020), 415–427.
[18] Z. J. Wang, X. Peng and F. Han, A novel time-event-driven algorithm for simulating spiking neural networks based on circular array, *Neurocomputing*, **292** (2018), 121–129.
[19] Q. Wang, X. Shi, and G. Chen, Delay-induced synchronization transition in small-world Hodgkin-Huxley neuronal networks with channel blocking, *Discrete Contin. Dyn. Syst. Ser. B*, **16** (2011), 607–621.
[20] B. Zhen, Z. Li and Z. Song, Influence of time delay in signal transmission on synchronization between two coupled FitzHugh-Nagumo neurons, *Applied Sciences*, **9** (2019), 2159.
[21] B. Zhen, D. Zhang and Z. Son, Complexity induced by external stimulations in a neural network system with time delay, *Math. Probl. Eng.*,**2020** (2020), 5472351, 9 pp.

Received December 2020; revised March 2021.

E-mail address: guxc@sdju.edu.cn
E-mail address: yadiahan@163.com
E-mail address: wangzj@dhu.edu.cn
E-mail address: kaleem@mail.dhu.edu.cn
E-mail address: wenlian@fudan.edu.cn